

LOW COST ALUMINIUM FOAMS MADE BY CaCO_3 PARTICULATES

Varužan Kevorkijan*

Independent Researcher, Betnavska cesta 6, 2000 Maribor, Slovenia

Received 09.09.2010

Accepted 05.10.2010

Abstract

In this work, the viability of CaCO_3 powder as a cost-effective alternative to TiH_2 foaming agent was investigated. Closed cell aluminium foam samples were prepared starting from solid, foamable precursors synthesized by (i) powder metallurgy and (ii) the melt route. Precursors obtained by the melt route were machined and additionally cold isostatically pressed in order to improve their density. In all cases, the resulting precursors consisted of an aluminium matrix containing various fractions (3, 5, 7 and 12 wt. %) of uniformly dispersed CaCO_3 powders of various average particle size (d_{50} = 38, 72 and 120 μm). Precursors were foamed by inserting them into a cylindrical stainless steel mould and placing them in a pre-heated batch furnace at 750 °C for 10 min.

The quality of the foamable precursors was evaluated by determining their initial density and the foaming efficiency (the relative density of the foam obtained, ρ , calculated by dividing the apparent density of the foam, ρ_F , by the density of aluminium, ρ_{Al}). In addition, the quality of the foams obtained was characterised by their density, microstructure (the average pore size) and mechanical properties (uniaxial room temperature compression stress-strain curve, compressive strength and energy absorption after a 30% strain).

The experimental findings confirmed that aluminium foams synthesized with CaCO_3 powder as a blowing agent can be prepared by both powder metallurgy and the melt route, as well as showing that the density, microstructure, compression strength and energy absorption capacity are quite comparable with the corresponding counterparts foamed by TiH_2 .

Key words: aluminium foams, foamable precursors, CaCO_3 powders

* Corresponding author: Varužan Kevorkijan, varuzan.kevorkijan@impol.si

Introduction

Closed cell foamed aluminium is a macro-composite material consisting of an aluminium alloy matrix, usually discontinuously reinforced with various ceramic particulates and closed pores filled with gas distributed throughout the matrix. This unique structure possesses an unusual combination of properties such as low density, high weight specific stiffness, extraordinary energy absorption and remarkable vibration attenuation, important for a number of engineering applications. Aluminium foams are also non-flammable, ecologically harmless and easily recyclable.

There are many possible applications for aluminium foams ranging from light-weight construction (foams can be used to optimize the weight-specific bending stiffness of engineering components), sound and heat insulation (foams can damp vibration and absorb sound) to energy absorption applications (during its deformation foams can absorb a large quantity of mechanical energy), acting as impact energy absorbers and lightweight ballistic structures.

Methods to produce closed cell aluminium foams have been known for a number of years and can be generally separated into two fundamental groups: (i) foaming liquid metal (casting procedures) and (ii) foaming metallic precursors (powder metallurgy-PM procedures)¹.

Titanium hydride (TiH_2) was mainly applied as blowing agent for both the casting and powder metallurgical procedures of foaming of aluminium and aluminium alloys. The role of the blowing agent in both casting and powder metallurgical procedures of foaming of aluminium is to release gas, since the metal is transferred in the liquid or the semi-liquid viscous state.

However, as foaming agent for the production of aluminium alloy foams by the casting and powder metallurgical routes, TiH_2 has several limitations that significantly influence the mass application of Al foams. The main limitations of foaming technologies using TiH_2 as foaming agent are the following:

- TiH_2 is expensive making such production less-competitive.
- The decomposition temperature of TiH_2 is very low – starting at about 400 °C for the untreated hydride – and commercial aluminium alloys have a solidus temperature above 525 °C. It is obvious that untreated TiH_2 does not match well the melting range of any of the Al alloys applied for foaming.
- Pre-treatment of TiH_2 by oxidation, which covers the surface of TiH_2 particles with a TiO_2 layer, or by other surface engineering techniques for creating specific protective layers (e.g. electroplating by nickel or sol-gel formation of a protective SiO_2 layer) was found to shift the decomposition range to higher temperatures. Although these procedures work well, they additionally increase the cost.
- TiH_2 particles act only as the blowing agent and are not involved in foam stability; therefore, if TiH_2 is applied, the addition of other solid particles (e.g. SiC) is necessary for bubble stabilisation, which also introduces an extra cost.
- The density of TiH_2 (approx. 3.9 g/cm³) is significantly higher than the density of molten aluminium (approx. 2.7 g/cm³). Thus, during foaming the settling of TiH_2 particles occurs by gravity, resulting in a non-uniform microstructure of the foam.

A cost-effective and highly promising alternative to TiH_2 blowing agent is CaCO_3 , as marble powder or synthetic calcium carbonate. In contrast to TiH_2 , calcium carbonate is of low cost, significantly lower than the cost of aluminium and with a

density (2.71 to 2.83 g/cm³) almost identical to the density of molten aluminium. Moreover, its decomposition temperature is above the melting point of aluminium, usually in the temperature interval between 660 °C and 930 °C. Therefore, CaCO₃ is particularly suitable for the melt-route settling-free production of foamed aluminium-based materials.

The “Foamcarp” process of indirect foaming of aluminium by CaCO₃ particles previously introduced into a solidified precursor and, more recently, an additional indirect foaming procedure of molten aluminium by a CaCO₃ - containing preform isostatically pressed from a mixture of CaCO₃ and AA6061 powders were reported^{2,3}.

In some early patents⁴ and in the recent work of Nakamura et al.⁵, the use of CaCO₃ was found to be potentially suitable as a foaming agent for direct (melt-route) foam manufacturing. Moreover, Bryat et al.⁶ reported that CaCO₃ acts in contact with molten aluminium as a foaming agent and, at the same time, through the decomposition products has a significant effect on foam stabilisation, enabling the formation of “self-stabilized aluminium foams” (i.e. foams solidified from a foamable suspension created through the controlled decomposition of carbonate powders with molten aluminium). A similar cell face stabilising mechanism operating in carbonate-foamed melts was also reported by Gergely et al.².

The additional advantage of CaCO₃ in comparison with TiH₂ blowing agent of the same average particle size is in achieving foams with higher porosity levels and finer cell sizes⁵. Gergely et al.² showed that replacing TiH₂ by CaCO₃ as foaming agent, foams can be produced having appreciably finer cells and more uniform cell structures at significantly reduced raw material cost.

Although the applicability of CaCO₃ powder as foaming agent in the direct and the indirect foaming of aluminium alloys and composites has already been investigated, there is a need for an additional study of the influence of the CaCO₃ powder morphology (particularly the average particle size and particle size distribution) and the role of CaCO₃ decomposition products on the achievement of better foam stability and a higher foam quality.

Hence, in this paper, the performance of synthetic calcium carbonate as a cost-effective foaming agent was investigated by both the powder metallurgical and the melt route of foam preparation. The influence of CaCO₃ particle morphology and volume fraction on foaming behaviour and the development of foam microstructure were also monitored. As result, a clearer interrelation between foam morphology and structure on the one hand, and its mechanical properties on the other, was established.

Experimental procedure

All the foams made in this work were prepared by indirect foaming methods starting from a solid foamable precursor consisting of a metallic matrix containing uniformly dispersed blowing agent particles. Foamable precursors were made by either: (i) the powder metallurgical route, or (ii) the melt route using the same blowing agent, i.e. CaCO₃ powders (types A, B and C) with various average particle sizes (38, 72 and 120 μm, respectively).

Following the powder metallurgical (PM) route, foamable precursors were made by mixing Al powder with an average particle size of 63 μm (purity: 99.7 wt. %, oxygen

content: 0.25 wt. %) and 3, 5, 7 and 12 wt. % of the blowing agent, followed by cold compaction in a lubricated 20 mm diameter die to a pressure of 600 to 900 MPa.

In the case of the melt route, foamable precursors with the same concentration of CaCO₃ blowing agent (3, 5, 7 and 12 wt. %) and the same geometry were prepared by an induction heated batch-type stir-casted method in which aluminium powder (the same as used for the PM route) was induction melted, followed by the addition of CaCO₃ particles, stirring and casting. Once the molten aluminium had reached 750 °C, the power was switched off and melt stirring was initiated until the temperature of the melt decreased to 700 °C. After that, the blowing agent/aluminium powder mixture (1:2 mass ratio) was introduced and the melt was stirred (at approximately 1200 rpm) for an additional 30-90 s. Finally, the foamable precursors were prepared by casting the semi-solid slurry into a room temperature mould with a 20 mm diameter.

The solidified precursors were machined and some of the samples were additionally cold isostatically pressed.

The density of the foamable precursors as well as the foams obtained was calculated from the mass and geometry of the samples and, in addition, measured by Archimedes' method. The distribution of blowing agent particles inside the Al matrix was examined by analysing the optical and scanning electron micrographs of as polished bars.

All precursors were foamed in a conventional batch furnace with air atmosphere circulation under the same experimental conditions (temperature, time, cooling method). Before foaming, the individual precursors were inserted into a cylindrical (40 mm in diameter, 70 mm long) stainless steel mould coated with a boron nitride suspension. The mould dimensions and the precursor size (20 mm in diameter and 60 mm long) were selected to allow expansion of the precursor to a foam with a theoretical density close to 0.6 g/cm³. The arrangement was placed inside a pre-heated batch furnace at 750 °C for 10 min. After that period of time, the mould was removed from the furnace and the foaming process was stopped by rapid cooling with pressurised air to room temperature. The thermal history of the foam sample was recorded, using a thermocouple located directly in the precursor material.

The porosity of the foam was calculated by the equation: $1 - (\text{foam density} / \text{aluminium density})$. Macro and microstructural examinations were performed on sections obtained by precision wire cutting across the samples and on samples mounted in epoxy resin, using optical and scanning electron microscopy (SEM-EDS).

The average particle size of pores in the foams was estimated by analysing the optical and scanning electron micrographs of as-polished foam bars using the point counting method and image analysis and processing software.

Regarding the mechanical properties of the foams, uniaxial room temperature compressive tests were carried out on a Zwick 1474 testing machine at a constant 5 mm/min crosshead displacement. Testing was performed on standard prismatic foam specimens of 50 mm x 12 mm x 17 mm so that each point of the stress-strain curve was determined as an average of four individual measurements. Compression was stopped whenever either 80% strain or 95 kN force (equivalent to 61.9 MPa) were reached. As a result of testing, the uniaxial compression stress-strain curve, compressive strength and energy absorption after a 30% strain were determined and correlated with the density, the average pore size and microstructure of the foam samples.

Results and discussion

Chemical reactivity of CaCO₃ with aluminium foam constituents

Foaming of aluminium alloys and aluminium-based composites with CaCO₃ blowing agent is caused by the thermal decomposition of calcium carbonate in contact with molten aluminium at temperatures above 700 °C. The overall chemical reaction is complex, consisting of several successive reactions which lead to the formation of various solid (CaO, Al₂O₃, Al₄C₃) and gaseous phases (CO₂, CO).

The decomposition of CaCO₃ is usually described by Reaction 1:

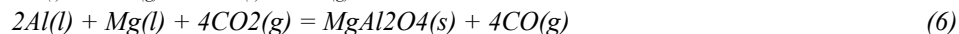
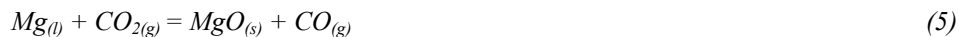


Theoretically, under normal atmospheric pressure the thermal decomposition of pure CaCO₃ is thermodynamically favourable only at temperatures above 900 °C. However, note that in the real system, chemical conversion occurs at the interface of CaCO₃ and liquid or semi-solid aluminium. Hence, in order to investigate the real process of foaming, additional chemical reactions should be also considered. Here, only three possible ones are listed, although several other are also reported²:



Reactions (2)-(4) are all thermodynamically favourable, even at temperatures significantly below the melting point of aluminium.

In addition, if magnesium as alloying element is present in the melt, MgO and MgAl₂O₄ solid phases are also formed according to Reactions 5 and 6:



At the foaming temperatures involved, the equilibrium CO₂ pressure over CaCO₃ is only a small fraction of the atmospheric pressure. This implies that melt foaming via CO₂ gas released from the carbonate is only possible if the partial pressure of CO₂ in the cell is maintained below its equilibrium value via the carbon dioxide-liquid metal reaction², leading to the formation of a metal oxide and carbon monoxide (Reaction 2).

The minimum fraction of CO₂ gas which is required to participate in the melt oxidation was theoretically analysed by Gergely et al.², showing that the thermal decomposition of less than 30% of the available carbonate should be sufficient for the production of high porosity foam.

Characterisation of the foamable precursors

Morphology of the applied foaming agent – calcium carbonate powder grade A is presented in Fig.1. As evident, calcium carbonate particles are non-agglomerated.

Moreover, XRD analysis of CaCO_3 powder (grade A), Fig. 2, approved its technical grade purity.

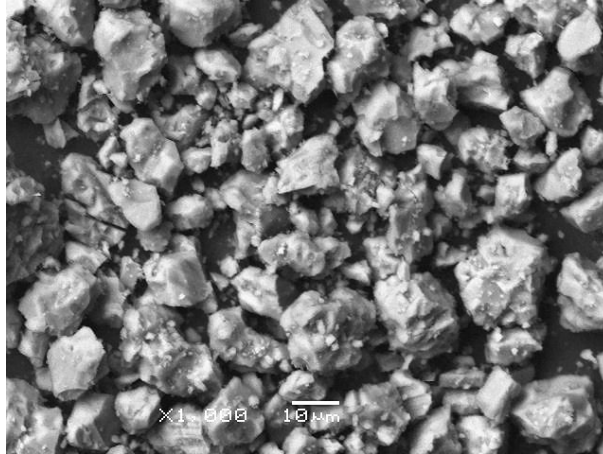


Fig. 1: SEM micrograph showing the size and morphology of the foaming agent – CaCO_3 powder grade A

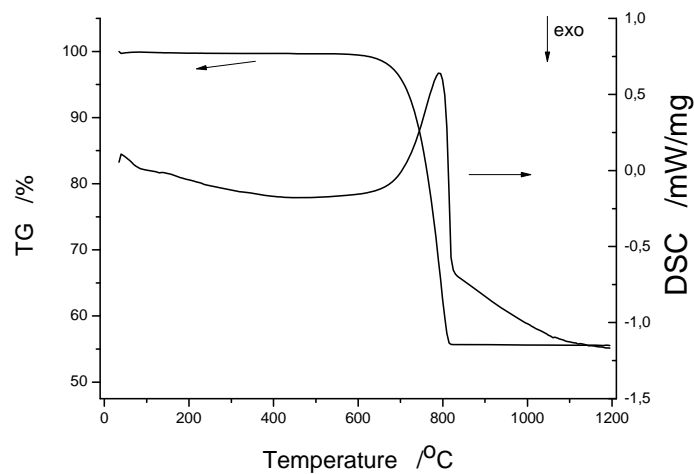


Fig.2: Thermogravimetric (TG) and differential scanning calorimetric (DSC) measurement curves for CaCO_3 powder grade A

Thermogravimetric (TG) and differential scanning calorimetric (DSC) measurement curves for CaCO_3 powder grade A are plotted in Fig. 3. TG analysis has shown that CaCO_3 undergoes thermal decomposition above approximately $650\text{ }^\circ\text{C}$ and the decomposition ends about $800\text{ }^\circ\text{C}$. Because of that, higher foaming temperatures are necessary than with TiH_2 , particularly when higher foaming efficiency on final foams is required. On the other side, higher onset temperature of CO_2 evolution from CaCO_3

powder enabling the incorporation of calcium carbonate particles into aluminium melt without the need of any special pre-treatment in order to prevent premature gas-release. However, as it was demonstrated by Gergely et al,^x thermal decomposition (chemical conversion) of less than 30% of the available carbonate in precursor should be sufficient for the production of high porosity (~95%) material. Fortunately, such a partial conversion could be easily achieved by holding the foaming precursors for a short period of time (5-10 min.) to temperature between 650 °C and 750 °C.

The measured and calculated densities of foamable precursors obtained by the PM route, Table 1, confirmed that under isostatic pressing with an applied pressure of 700 MPa the precursors prepared by PM possessed closed porosity and densities above 98% of theoretical, whereas as-machined precursors obtained by the melt route, Table 2, had a significant fraction of open porosity and thus were not suitable for foaming to the desired foam densities (usually about 0.5 to 0.7 g/cm³). However, after an additional isostatic pressing, the porosity in these precursors was successfully reduced below 2.0 vol. %, Table 3, enabling preparation of foam samples with densities between 0.62 g/cm³ and 0.80 g/cm³.

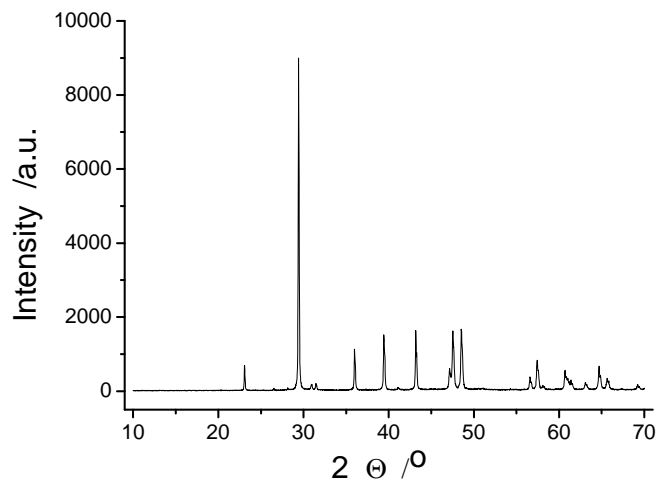


Fig.3: XRD of CaCO₃ powder (grade A)

It is important to note that very high precursor densities (>99% of theoretical) were achieved only in precursors prepared by the powder metallurgical route with 3-7% of CaCO₃ particles of Type-A, Table 1. With a higher particle content, and by use of coarser CaCO₃ powders of Type-B or Type-C, this could not be achieved, resulting in a lower foaming efficiency, as evident in Tables 4-6.

The foaming efficiency of precursors was evaluated based on the relative density of the foam obtained, ρ , calculated by dividing the apparent density of the foam, ρ_F , by the density of aluminium, ρ_{Al} . Thus, the foaming efficiency is expressed as:

$$\eta = 1 - \rho = 1 - (\rho_F / \rho_{Al}) \quad (7)$$

which actually corresponds to the volume fraction of pores in the foam samples. The lower the foam density, the higher is the foaming efficiency.

Table 1: Porosity of foamable precursors obtained by the PM route

Chemical composition of precursors (wt. %)		Porosity (vol. %)	
CaCO ₃	Al powder	Calculated	Measured
Type-A			
3	97	0.8±0.08	0.7±0.04
5	95	0.8±0.08	0.8±0.04
7	93	0.9±0.09	1.0±0.05
10	90	1.1±0.11	1.2±0.06
Type-B			
3	97	1.1±0.10	1.0±0.05
5	95	1.1±0.11	1.1±0.06
7	93	1.3±0.13	1.3 ±0.07
10	90	1.7±0.17	1.8±0.09
Type-C			
3	97	1.3±0.11	1.4±0.07
5	95	1.5±0.15	1.4±0.07
7	93	1.6±0.16	1.7±0.09
10	90	1.8±0.18	2.0±0.10

Table 2: Porosity of as-machined foamable precursors prepared by the melt route

Chemical composition of precursors (wt. %)		Porosity (vol. %)	
CaCO ₃	Al powder	Calculated	Measured
Type-A			
3	97	4.2±0.42	4.1±0.21
5	95	4.6±0.46	4.4±0.22
7	93	4.9±0.49	4.8±0.24
10	90	5.3±0.53	5.2±0.26
Type-B			
3	97	4.1±0.41	4.2±0.21
5	95	4.7±0.47	4.7±0.24
7	93	5.0±0.50	5.1±0.26
10	90	5.4±0.54	5.5±0.28
Type-C			
3	97	3.9±0.39	4.1±0.21
5	95	4.2±0.42	4.2±0.21
7	93	4.3±0.43	4.4±0.22
10	90	4.8±0.48	4.9±0.25

Table 3: Porosity of foamable precursors obtained by the melt route improved by additional isostatic pressing

Chemical composition of precursors (wt. %)		Porosity (vol. %)	
CaCO ₃	Al powder	Calculated	Measured
Type-A			
3	97	1.3±0.13	1.3±0.06
5	95	1.6±0.16	1.7±0.09
7	93	1.9±0.19	2.0±0.10
10	90	2.0±0.20	2.2±0.11
Type-B			
3	97	1.1±0.11	1.2±0.06
5	95	1.2±0.12	1.2±0.06
7	93	1.4±0.14	1.5±0.08
10	90	1.7±0.17	1.9±0.09
Type-C			
3	97	1.0±0.10	1.0±0.10
5	95	1.2±0.12	1.1±0.06
7	93	1.3±0.13	1.4±0.07
10	90	1.6±0.16	1.8±0.09

Table 4: Density, foaming efficiency and average pore size of aluminium foams prepared by the PM route

Initial composition of foamable precursors (wt. %)		Selected properties of foamed samples		
CaCO ₃	Al powder	Density (g/cm ³)	Foaming efficiency (%)	Average pore size (mm)
Type-A				
3	97	0.42±0.02	84.4	0.8±0.08
5	95	0.47±0.03	82.6	0.9±0.09
7	93	0.51±0.03	81.1	1.0±0.10
10	90	0.55±0.03	79.6	1.2±0.12
Type-B				
3	97	0.46±0.03	83.0	0.5±0.05
5	95	0.49±0.03	81.9	0.7±0.07
7	93	0.53±0.03	80.4	0.8±0.08
10	90	0.59±0.03	78.1	0.9±0.09
Type-C				
3	97	0.53±0.03	80.4	0.5±0.05
5	95	0.55±0.03	79.6	0.5±0.05
7	93	0.59±0.03	78.1	0.6±0.06
10	90	0.61±0.03	77.4	0.8±0.08

Table 5: Density, foaming efficiency and average pore size of aluminium foams prepared from as-machined foamable preforms fabricated by the melt route

Initial composition of foamable precursors (wt. %)		Selected properties of foamed samples		
CaCO ₃	Al powder	Density (g/cm ³)	Foaming efficiency (%)	Average pore size (mm)
Type-A				
3	97	0.89±0.05	67.0	1.1±0.11
5	95	0.92±0.05	65.0	1.3±0.13
7	93	0.97±0.05	64.1	1.4±0.14
10	90	0.99±0.05	63.3	1.4±0.14
Type-B				
3	97	0.84±0.03	68.9	0.8±0.08
5	95	0.89±0.03	67.0	0.9±0.09
7	93	0.93±0.04	65.6	0.9±0.09
10	90	0.95±0.04	64.8	1.1±0.11
Type-C				
3	97	0.79±0.04	70.7	0.7±0.07
5	95	0.81±0.04	70.0	0.8±0.08
7	93	0.85±0.04	68.5	1.2 ±0.12
10	90	0.88±0.04	67.4	1.5±0.15

Table 6: Density, foaming efficiency and average pore size of aluminium foams prepared by the melt route from as-machined and additionally isostatically pressed foamable precursors

Initial composition of foamable precursors (wt. %)		Selected properties of foamed samples		
CaCO ₃	Al powder	Density (g/cm ³)	Foaming efficiency (%)	Average pore size (mm)
Type-A				
3	97	0.69±0.03	74.4	1.1±0.11
5	95	0.72±0.04	73.3	1.2±0.12
7	93	0.76±0.04	71.9	1.3±0.13
10	90	0.80±0.04	70.4	1.6±0.16
Type-B				
3	97	0.64±0.03	76.3	0.8±0.08
5	95	0.69±0.03	74.4	0.9±0.09
7	93	0.72±0.04	73.3	1.3±0.13
10	90	0.74±0.04	72.6	1.4±0.14
Type-C				
3	97	0.62±0.03	77.0	0.9±0.09
5	95	0.67±0.03	75.2	1.1±0.11
7	93	0.71±0.04	73.7	1.3 ±0.13
10	90	0.73±0.04	73.0	1.6±0.16

In all cases, the experimental results clearly indicate that the porosity measured in foamable precursors and the apparent densities achieved in aluminium foam samples are inversely proportional. Generally, foamable precursors with lower porosity resulted in foam samples with higher apparent density and lower foaming efficiency.

Under the same foaming conditions (temperature, time), the average pore size of foam samples was influenced by the density of the foaming precursors and the initial size of the foaming particles. As a rule, in foams made from precursors with high density ($\geq 99\%$ of theoretical), the average pore size remained below 1.0 mm. On the other hand, in foams made from precursors with lower density (below 99% of theoretical), pores grew to a 20 to 50% higher average pore size.

Regarding the initial size of the foaming particles, which also influences the density of the precursor and hence the density of the foam samples, an increase of the average particle size of the CaCO₃ foaming agent was observed to have a detrimental influence on the average size of pores. Coarser CaCO₃ powders led to the formation of larger bubbles in the foam structure.

Microstructural investigation of aluminium foam samples

Similar cellular structural development with spherical, closed pores was obtained by both powder metallurgy, Fig. 4, and the melt processing route, Fig. 5. However, as evident in Fig. 4, the samples obtained by the powder metallurgical route had a more uniform microstructure consisting of well separated individual cells. On the other hand, the microstructure of samples obtained by the melt processing route, Fig. 5, revealed the presence of some individual non-uniformities created by flow (the movement of bubbles with respect to each other), drainage (flow of liquid metal through the intersection of three foam films), coalescence (sudden instability in a foam film) and coarsening (slow diffusion of gas from smaller bubbles to larger ones).

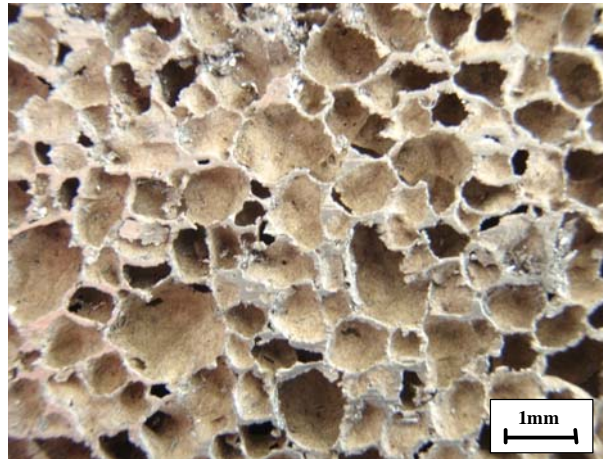


Fig. 4: Cross section of an aluminium foam obtained by the powder metallurgical route with well separated individual cells and relatively uniform microstructure.

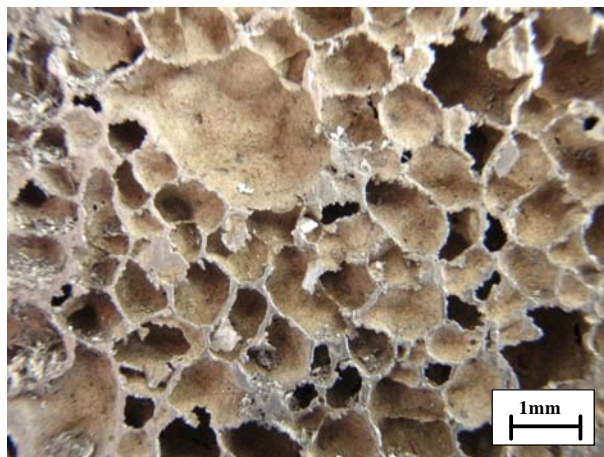


Fig. 5: Cross section of an aluminium foam obtained by the melt route with a characteristic channel network and foam drainage.

The absence of considerable pore coarsening and drainage suggests that there is a cell face stabilising mechanism operating in the carbonate-foamed melts², slowing down the cell face rupturing process and hence inhibiting cell coarsening. The mechanism is likely to be a result of the foaming gas (CO₂)/melt or semi-solid slurry reaction during the foaming procedure, as was discussed in detail by Gergely et al.².

Concerning the average pore size and the uniformity in cell size distribution, foams made by the powder metallurgical route have finer pores and more regular morphology than samples made by the melt route, particularly those from as-machined precursors. However, an additional cold isostatic pressing of the as-machined precursor obtained by the melt route was found to help in achieving more uniform foams with smaller average pore size, similar to those obtained by the powder metallurgical route. The improvement is most probably caused by better compacting of individual CaCO₃ particles and the aluminium matrix, resulting in a higher density of the foamable precursor.

Mechanical properties

Fig. 6 shows an example of the stress-strain response of samples foamed from preforms prepared by the PM route in which the compressive strength of the foams was correlated with their density.

Because of the closed cell structure, the compressive foam behaviour in all cases showed a typical stress-strain diagram with division into three parts: a linear increase in strength mainly caused by elastic deformation, followed by a plateau caused by homogeneous plastic deformation and a final steep increase due to collapse of the cells. The compressive strength was taken as the initial peak stress. Foams made by the PM route possessed the highest compressive strength, while samples foamed from as-machined precursors had significantly lower values. For the interval of foam densities analysed in this work (from 0.42 to 0.55 g/cm³), it was found that in more dense foam samples the position of the plateau shifted toward higher stress values.

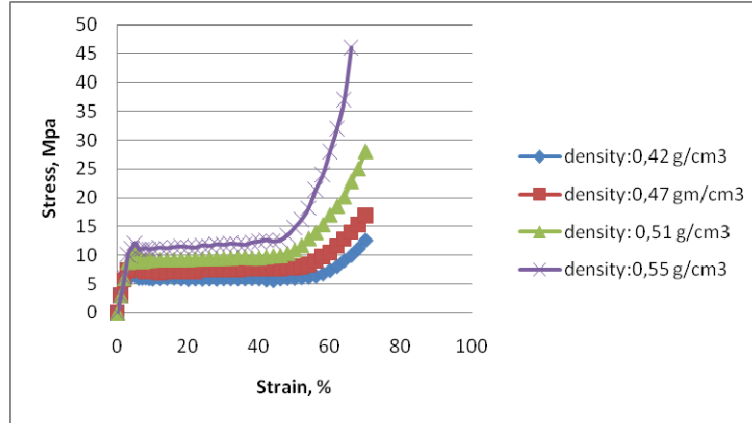


Fig. 6: The stress-strain response of various aluminium foam samples from preforms obtained by the PM route.

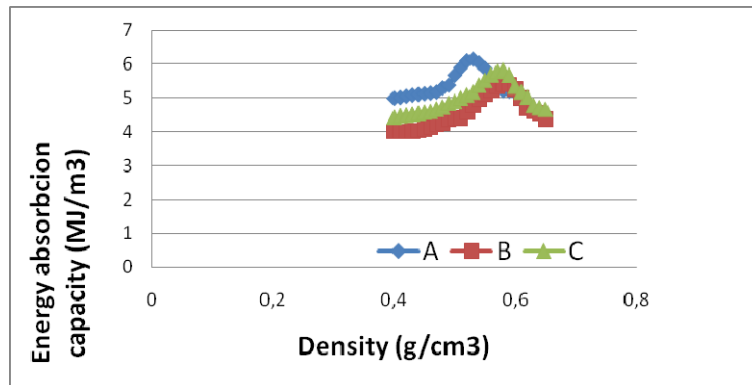


Fig. 7: Example of the optimization of aluminium foam density range for maximum energy absorption capacity: A)-foams obtained by powder metallurgy, B)-foams obtained from as-machined precursors fabricated by the melt route, and C)-foams obtained from as-machined and cold isostatically pressed precursors fabricated by the melt route.

The energy absorbed per unit volume (E-energy absorption capacity), which is one of the most important characteristics of aluminium foams, was determined by the area under the stress-strain plots as follows⁶:

$$E = \int_0^l \sigma(\epsilon) d\epsilon$$

where σ is compressive stress, l is the limit of strain concerned and ϵ is compressive strain. The calculated values of energy absorption capacity for samples are plotted in Fig. 6 and correlated with foam density. The typical response was found to be a quasi-Gaussian function with a maximum energy absorption capacity in a very narrow density range.

The maximum energy absorption capacity for various foams is summarized in Fig. 7. For foams made by the PM route, the maximum energy absorption capacity of 6.14 MJ/m^3 was achieved in foams with a density of 0.53 g/cm^3 . On the other hand, in samples foamed from as-machined precursors fabricated by the melt route, a maximum energy absorption capacity of only 5.41 MJ/m^3 was found. The maximum appeared at a foam density of 0.58 g/cm^3 . Finally, in melt route fabricated precursors, additionally isostatically pressed before foaming, an intermediate maximum energy absorption capacity of 5.82 MJ/m^3 was found in samples with a density of 0.58 g/cm^3 .

The foaming process does not materially affect the properties of the cell-wall material. However, it leads to a unique spatial distribution of aluminium which results in significantly different properties of the foamed component in comparison with the bulk part. It is obvious that the properties of aluminium foam significantly depend on its porosity, so that a desired property (or combination of properties) can be tailored by selecting the foam density.

The mechanical properties of foams obtained by applying dolomite powder as foaming agent are fully comparable with the corresponding properties of foams fabricated using TiH_2 .

Conclusion

The following conclusions can be drawn from this work.

- TiH_2 powder as foaming agent was successfully replaced by commercial CaCO_3 powders of different average particle size (38, 72 and $120 \mu\text{m}$, respectively.)
- Foaming precursors with different proportions (3-10 vol. %) of CaCO_3 powder particles as foaming agent were routinely prepared either by the powder metallurgical or melt route.
- Precursors obtained by powder metallurgy had superior homogeneity and densities $\geq 98\%$ of theoretical. Moreover, in precursors obtained by the PM route containing 3-7 vol. % of CaCO_3 particles of an average particle size of $38 \mu\text{m}$, densities $\geq 99\%$ of theoretical were achieved.
- With greater addition of CaCO_3 particles and by using CaCO_3 powders with higher average particle size (76 and $97 \mu\text{m}$), densities $\geq 99\%$ of theoretical could not be achieved.
- The foaming efficiency of experimentally prepared precursors was evaluated based on the relative density of the foams obtained (the apparent density of the foam divided by the density of aluminium). The experimental findings showed that the apparent density of foam samples is inversely proportional to the density of the foaming precursor. Thus, foamable precursors with higher density resulted in foam samples with lower apparent density and higher foaming efficiency. On the other hand, the foaming efficiency and the average pore size of foamed samples are generally reciprocally dependent. Thus, a higher foaming efficiency results in a foam microstructure with finer pores.
- The mechanical properties (compression strength and energy absorption capacity) of foamed samples are also strongly influenced by foaming efficiency. For the range of foam densities analysed, the compression strength, considered as the initial peak stress, was found to be superior (approx. 13 MPa) in samples with increased density (0.55 g/cm^3) and hence lower foaming efficiency (79.6%). In contrast to

this, the maximum energy absorption capacity was achieved in foams with the highest foaming efficiency.

- From the experimental findings is obvious that the properties of an aluminium foam significantly depend on its porosity, so that a desired property (or combination of properties) can be tailored by the foam density.
- The experimental findings confirm that the microstructure, compression strength and energy absorption capacity of aluminium foams prepared with CaCO₃ powder as foaming agent are quite comparable with their counterparts foamed by TiH₂.

Acknowledgement

This work was supported by funding from the Public Agency for Research and Development of the Republic of Slovenia, as well as the Impol Aluminium Company and Bistral d.o.o. from Slovenska Bistrica under contract No. 2410-0206-09.

Reference

- [1] J. Banhart, *Adv. Eng. Mater.* 8 (2006) 9, 781
- [2] V. Gergely, D. C. Curra, T. W. Clyne, *Composites Science and Technology* 63 (2003) 2301
- [3] L.E. G. Cambroner, J. M. Ruiz-Roman, F. A. Corpas, J. M. Ruiz Prieto, *Journal of Materials Processing Technology* 209 (2009) 1803
- [4] US Patent No. 2.751.289, issued June 19, 1956
- [5] T. Nakamura, S. V. Gbyloskurenko, K. Savanto, A. V. Byakova, R. Ishikawa, *Mater. Trans.* 43 (2002) 5, 1191-1196
- [6] J. D. Bryant, M. D. Clowley, M. D. Wilhelmy, J. A. Kallivayalil, W. Wang, In *Metfoam 2007*, DEStech Publications, Inc., Lancaster, PA, 2008, pp. 27
- [7] S. Asavavisithchai, R. Tantisiriphaiboon, *Chiang Mai J. Sci.* 36 (2009) 3, 302